Electronic Supplementary Material (ESI) for Dalton Transactions.

Supporting Information

Multicolour lanthanide(III) 1D coordination polymers: Tunable wide spectrum emission and efficient Cu^{II} ion sensing

Sanchita Karmkar[a#], Adrija Ghosh[b#], Komal Prasad[b], Faruk Ahamed Rahimi[a], Darsi Rambabu[a], Ritesh Haldar[bc] and Tapas Kumar Maji[ab]*

[a]Chemistry and Physics of Materials Unit (CPMU), [b]New Chemistry Unit (NCU), School of Advanced Materials (SaMat), Jawaharlal Nehru Centre for Advanced Scientific Research, Bangalore-560064, India; [c]Tata Institute of Fundamental Research Hyderabad, Gopanpally, Hyderabad 500064, Telengana, India

*E-mail: tmaji@jncasr.ac.in, URL: www.jncasr.ac.in/tmaji

Experimental Section

X-ray Crystallography

X-ray single crystal structural data of **2** (CCDC 1438262) was collected on a Bruker Smart-CCD diffractometer equipped with a normal focus, 2.4 kW sealed tube X-ray source with graphite monochromated Mo-Kα radiation (λ = 0.71073 Å) operating at 50 kV and 30 mA. The program SAINT[1] was used for integration of diffraction profiles and absorption correction was made with SADABS[2] program. All the structures were solved by SIR 92[3] and refined by the full matrix least-squares method using SHELXL-97.[4] All the hydrogen atoms were fixed by HFIX and placed in ideal positions. Potential solvent accessible area or void space was calculated using the PLATON multipurpose crystallographic software.[5] All crystallographic and structure refinement data of **2** is summarized in Table S1. Selected bond lengths and angles for **2** are given in Table S2-S3. All calculations were carried out using PLATON and WinGX system, Ver 1.70.01.[6]

Adsorption Measurements

Adsorption isotherms of N_2 (77 K and 195 K) and CO_2 (195 K) were recorded using the desolvated sample of **2** (**2′**) by using a QUANTACHROME QUADRASORB-SI analyzer. In the sample tube, the adsorbent sample (**2′**) (100−150 mg) were placed which had been prepared at 180 °C under a 1×10^{-1} Pa vacuum for about 12 h prior to measurement of the isotherms. Helium gas (99.999% purity) at a certain pressure was introduced in the gas chamber and allowed to diffuse into the sample chamber by opening the valve. The amount of gas adsorbed was calculated from the pressure difference ($P_{\mathrm{cal}}- P_{\mathrm{e}}$), where P_{cal} is the calculated pressure with no gas adsorption and P_{e} is the observed equilibrium pressure. All the operations were computer controlled and automatic.

Syntheses

Synthesis of 4,4′,4″-[1,3,5-phenyl-tri(methoxy)]-tris-benzoic acid (H_3L):

4,4′,4″-[1,3,5-phenyl-tri(methoxy)]-tris-benzoic acid was prepared following a reported procedure.[7] Methyl-4-hydroxy benzoate (1 g, 6.57 mmol), potassium carbonate (2.890 g, 20.1 mmol), and potassium iodide (0.085 g, 0.51 mmol) were heated in 30 mL DMF at 100 °C for 2 h in a nitrogen atmosphere. A solution of 1,3,5-tris(bromomethyl)benzene (0.500 g, 1.4 mmol) in 20 mL DMF was then added dropwise to the above-mentioned heated mixture. The mixture was then heated for 4 h at 100 °C. After cooling to room temperature, 100 mL of distilled water was added to it. The precipitate formed was filtered, washed with cold distilled water and air-dried to get a white solid of 4,4′,4″-[1,3,5-phenyl-tri(methoxy)]-tri-methyl benzoate. To 4,4′,4″-[1,3,5-phenyl-tri(methoxy)]-tri-methyl benzoate (for ~500 mg) 40 mL of MeOH and 1 g of sodium hydroxide dissolved in 10 mL of water was added in an RBF. The reaction mixture was then stirred at 50 °C for 12 h. After cooling to room temperature, the solution was placed in an ice bath and acidified with 6 N hydrochloric acid. The precipitate formed was then filtered, washed with cold distilled water and dried. The brownish solid of 4,4′,4″-[1,3,5-phenyl-tri(methoxy)]-tris-benzoic acid ligand was characterized by ^{1}H-NMR (Fig. S1). ^{1}H NMR (400 MHz, DMSOd6): δ 7.9 (d, J = 8.0 Hz, 6 H), 7.5 (s, J = 8.0 Hz, 3 H), 7.1 (d, J= 8.0 Hz, 6 H), 5.3 (s, J= 8.0 Hz, 6 H).

Syntheses of $\{[Tb_{(1-x)}Eu_x(L)(DMF)(H_2O)]\cdot 1.5H_2O\}_n$ (x= 0.0001 (1a), 0.059 (1b), 0.067 (1c), 0.075 (1d), 0.184 (1e) and 0.378 (1f))

The synthesis followed the similar procedure as that of compound **1**; just by replacing a certain amount of aqueous solution of $Tb(NO_3)_3\cdot 5H_2O$ with $Eu(NO_3)_3\cdot 5H_2O$ solution and keeping the total molar amount of the metal same (i.e. 0.75 mL of 10^{-5} M aqueous solution). We tried different combinations; 95%Tb^{III}-5%Eu^{III}, 90%Tb^{III}-10%Eu^{III}, 87%Tb^{III}-13%Eu^{III}, 85%Tb^{III}-15%Eu^{III}, 70%Tb^{III}-30%Eu^{III}, 50%Tb^{III}-50%Eu^{III}. Six different Eu^{III} doped Tb^{III} framework containing 37.8, 18.4, 7.5, 6.7, 5.9 and 0.01 atom% of Eu^{III} was prepared. Yield for **1a**: 69 %; Anal. Calcd. for $C_{66}H_{65}N_2O_{25}Tb_{1.9998}Eu_{0.0002}$: C, 49.56; H, 4.06; N, 1.75. Found C, 48.540; H, 4.072; N, 2.012. FT-IR (KBr pellet, 4000–400 cm^{-1}): 3346 (b), 3074 (w), 2925 (s), 1560 (m), 1509 (s), 1312 (s), 1276 (w), 1252 (s), 1222 (s), 1170 (s), 1143 (m), 1107 (s), 1041 (s), 1006 (s), 911 (w), 865 (s), 852 (w), 787 (s), 727 (s), 700 (s), 674 (s), 646 (w), 622 (w), 612 (s), 562 (s), 435 (w). Yield for **1b**: 78 %; Anal. Calcd.for $C_{66}H_{65}N_2O_{25}Tb_{1.882}Eu_{0.118}$: C, 49.57; H, 4.07; N, 1.75. Found C, 48.540; H, 4.072; N, 2.012. FT-IR (KBr pellet, 4000–400 cm^{-1}): 3346 (b), 3074 (w), 2925 (s), 1560 (m), 1509 (s), 1312 (s), 1276 (w), 1252 (s), 1222 (s), 1170 (s), 1143 (m), 1107 (s), 1040 (s), 1009 (s), 911 (w), 866 (s), 852 (w), 787 (s), 727 (s), 700 (s), 674 (s), 646 (w), 622 (w), 612 (s), 562 (s), 435 (w). Yield for **1c**: 75 %; Anal. Calcd.for $C_{66}H_{65}N_2O_{25}Tb_{1.866}Eu_{0.134}$: C, 49.57; H, 4.07; N, 1.75. Found C, 48.753; H, 4.29; N, 1.85. FT-IR (KBr pellet, 4000–400 cm^{-1}): 3343 (b), 3071 (w), 2925 (s), 1560 (m), 1509 (s), 1312 (s), 1276 (w), 1252 (s), 1222 (s), 1170 (s), 1143 (m), 1102 (s), 1041 (s), 1006 (s), 911 (w), 865 (s), 852 (w), 789 (s), 727 (s), 701 (s), 674 (s), 646 (w), 622 (w), 612 (s), 562 (s), 435 (w). Yield for **1d**: 72 %; Anal. Calcd.for $C_{66}H_{65}N_2O_{25}Tb_{1.85}Eu_{0.15}$: C, 49.57; H, 4.07;

N, 1.75. Found C, 48.782; H, 4.30; N, 1.902. FT-IR (KBr pellet, 4000−400 cm^{-1}): 3345 (b), 3074 (w), 2926 (s), 1562 (m), 1509 (s), 1312 (s), 1276 (w), 1252 (s), 1222 (s), 1170 (s), 1143 (m), 1107 (s), 1041 (s), 1006 (s), 911 (w), 865 (s), 852 (w), 787 (s), 727 (s), 700 (s), 674 (s), 646 (w), 622 (w), 612 (s), 562 (s), 435 (w). Yield for **1e**: 68 %; Anal. Calcd.for $C_{66}H_{65}N_2O_{25}Tb_{1.632}Eu_{0.368}$: C, 49.7; H, 4.07; N, 1.75. Found C, 49.64; H, 4.46; N, 1.79. FT-IR (KBr pellet, 4000−400 cm^{-1}): 3346 (b), 3074 (w), 2925 (s), 1560 (m), 1509 (s), 1312 (s), 1276 (w), 1252 (s), 1223 (s), 1170 (s), 1143 (m), 1107 (s), 1041 (s), 1006 (s), 911 (w), 865 (s), 852 (w), 787 (s), 727 (s), 701 (s), 674 (s), 645 (w), 624 (w), 612 (s), 562 (s), 435 (w). Yield for **1f**: 77 %; Anal. Calcd.for $C_{66}H_{65}N_2O_{25}Tb_{1.244}Eu_{0.756}$: C, 49.75; H, 4.07; N, 1.75. Found C, 48.723; H, 4.38; N, 1.76. FT-IR (KBr pellet, 4000−400 cm^{-1}): 3347 (b), 3074 (w), 2926 (s), 1560 (m), 1509 (s), 1316 (s), 1276 (w), 1252 (s), 1223 (s), 1170 (s), 1143 (m), 1107 (s), 1043 (s), 1006 (s), 911 (w), 864 (s), 852 (w), 787 (s), 727 (s), 700 (s), 674 (s), 646 (w), 622 (w), 612 (s), 562 (s), 435 (w).

Table S1: Crystal data and structure refinement parameters of **2**.

Parameters	**2**
Empirical formula	$C_{66}H_{65}N_2O_{25}Eu_2$
Formula weight	1590.11
Crystal system	Triclinic
Space group	$P\bar{1}$
a, Å	8.5690(5)
b, Å	14.4339(8)
c, Å	14.4711(9)
α, deg	98.739(4)
β, deg	95.779(4)
γ, deg	106.745(4)
V, Å^3	1674.20(18)
Z	1
T, K	294
μ,mm^{-1}	1.938
D_{calcd},g/cm^3	1.576
F (000)	800

Reflections [$I>2\sigma(I)$]	3295
Unique reflections	6561
Total reflections	19721
R_{int}	0.178
GOF on F^2	0.99
$R_1[I>2\sigma(I)]^a$	0.0794
R_w[all data]^b	0.1922
$\Delta\rho$ max/min [e Å^{-3}]	0.97, -1.11

${}^aR_1= \sum||F_o|-|F_c||/\sum|F_o|$;${}^bR_w= [\sum\{w(F_o^2-F_c^2)^2\}/\sum\{w(F_o^2)^2\}]^{1/2}$

Table S2: Selected Bond Distances (Å) for **2**.

Eu-O1	2.440(9)	Eu-O4	2.466(9)
Eu-O1W	2.424(9)	Eu-O5	2.295(10)
Eu-O2	2.496(7)	Eu-O7	2.426(11)
Eu-O3	2.447(9)	Eu-O6_c	2.373(9)

Symmetry code, c= -x,-y,-z

Table S3: Selected bond angles (°) for **2**.

O1-Eu-O1W	79.4(3)	O1-Eu-O2	52.9(3)
O4-Eu-O6_c	75.2(3)	O1-Eu-O3	115.2(3)
O5-Eu-O7	152.8(4)	O1-Eu-O4	139.9(3)
O1-Eu-O5	90.0(3)	O5-Eu-O6_c	109.0(3)
O1-Eu-O7	74.3(3)	O6_c-Eu-O7	75.7(4)
O1-Eu-O6_c	144.5(3)	O1W-Eu-O2	126.2(3)
O1W-Eu-O3	153.0(3)	O1W-Eu-O4	129.7(3)
O1W-Eu-O5	74.9(3)	O1W-Eu-O7	80.4(3)
O1W-Eu-O6_c	77.3(3)	O2-Eu-O3	78.3(3)
O2-Eu-O4	87.7(3)	O2-Eu-O5	81.3(3)
O2-Eu-O7	105.1(3)	O2-Eu-O6_c	156.5(3)
O3-Eu-O4	53.3(3)	O3-Eu-O5	125.1(3)

O3-Eu-O7	82.0(3)	O3-Eu-O6_c	78.6(3)
O4-Eu-O5	75.6(3)	O4-Eu-O7	130.3(3)

Symmetry code, c= -x,-y,-z

Table S4: Structural parameters of compound **1** obtained after Profile matching.

Parameters	1
a, Å	8.5433(4)
b, Å	14.3905(8)
c, Å	14.5241(8)
α, deg	99.1208(6)
β, deg	95.708(3)
γ, deg	107.024(3)
V, Å³	1665.55(17)

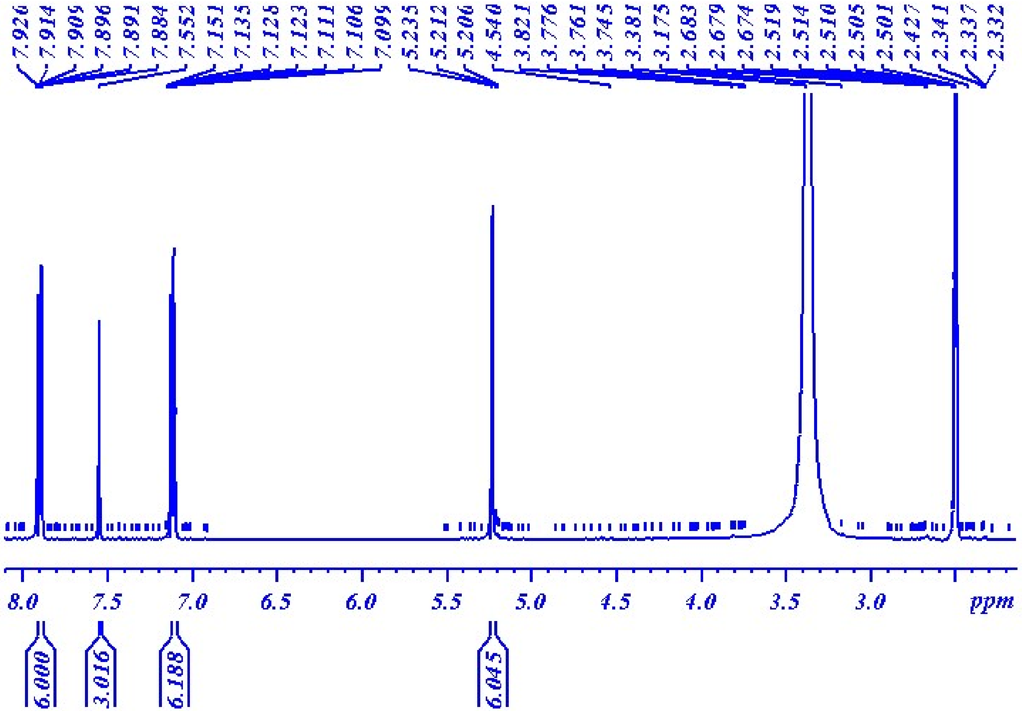

Fig.S1: ^{1}H-NMR of 4,4′,4″-[1,3,5-phenyl-tri(methoxy)]-tris-benzoic acid in D_6-DMSO.

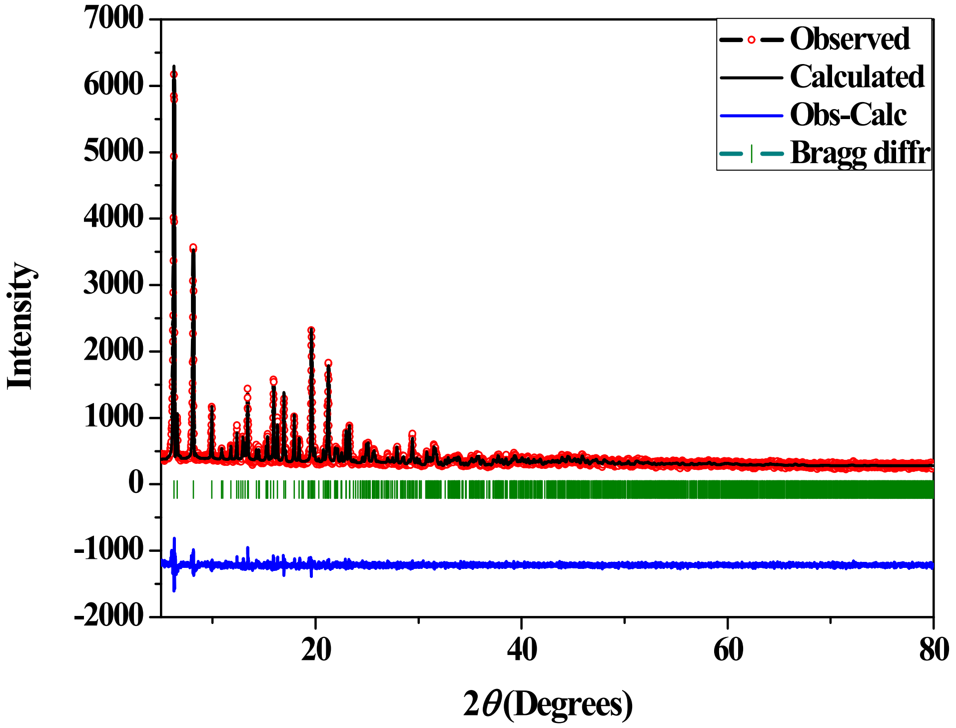

Fig.S2: Pattern matching for powder X-ray diffraction profile of compound **1**.

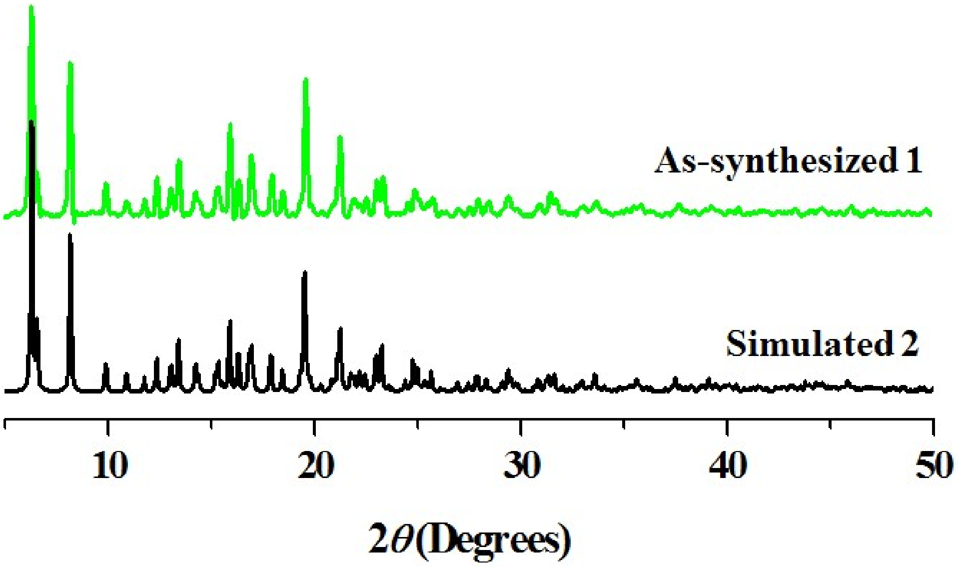

Fig.S3: PXRD pattern of phase pure compound **1**.

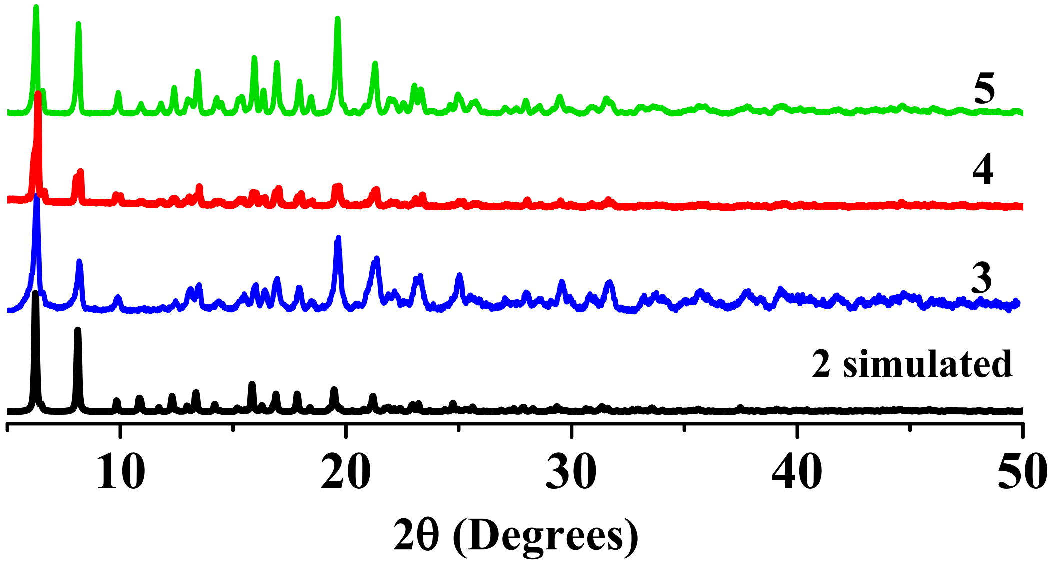

Fig.S4: PXRD patterns of simulated 1 compound and **3**, **4** and **5** compounds.

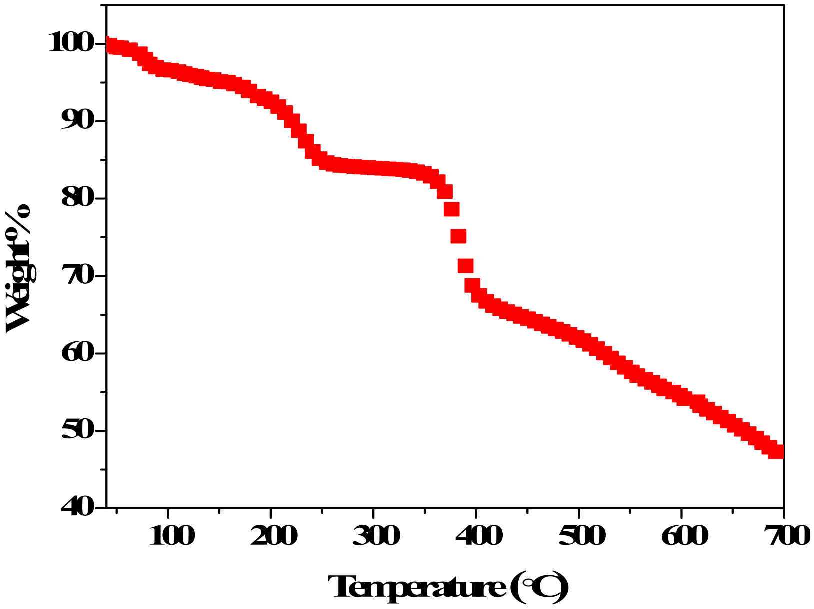

Fig.S5: TGA profile of compound **2**.

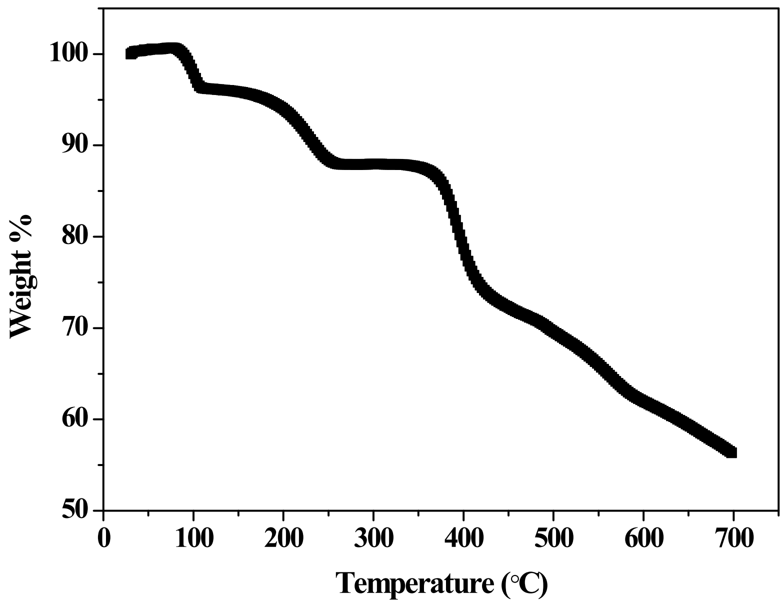

Fig.S6: TGA profile of compound **1**.

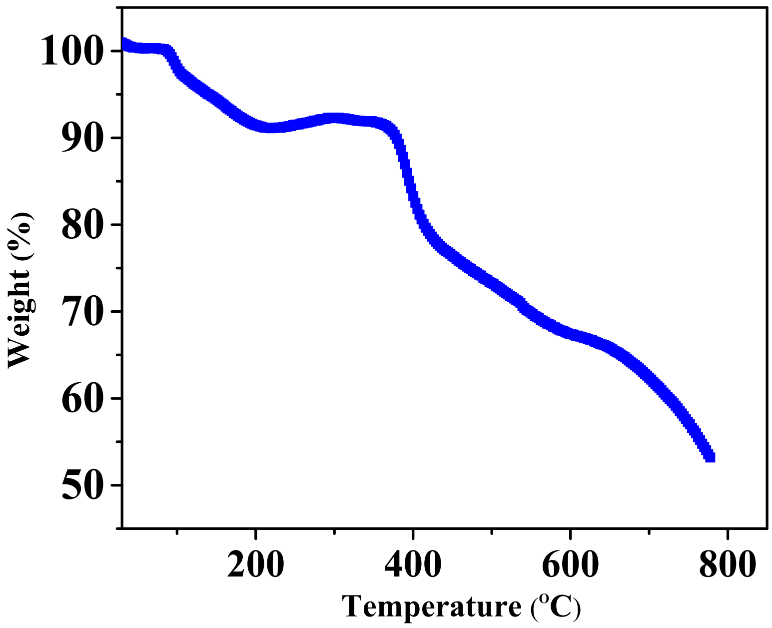

Fig. S7 TGA of compound 3

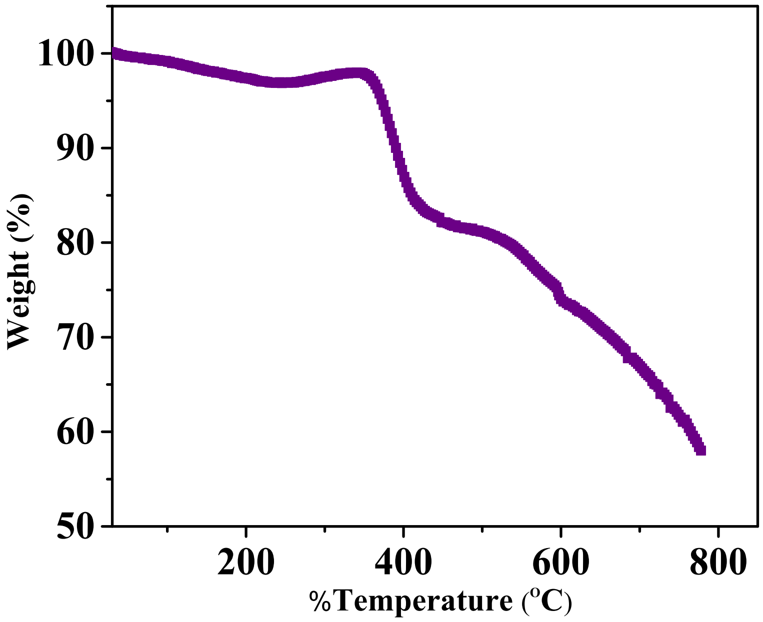

Fig. S8 TGA of compound **4**

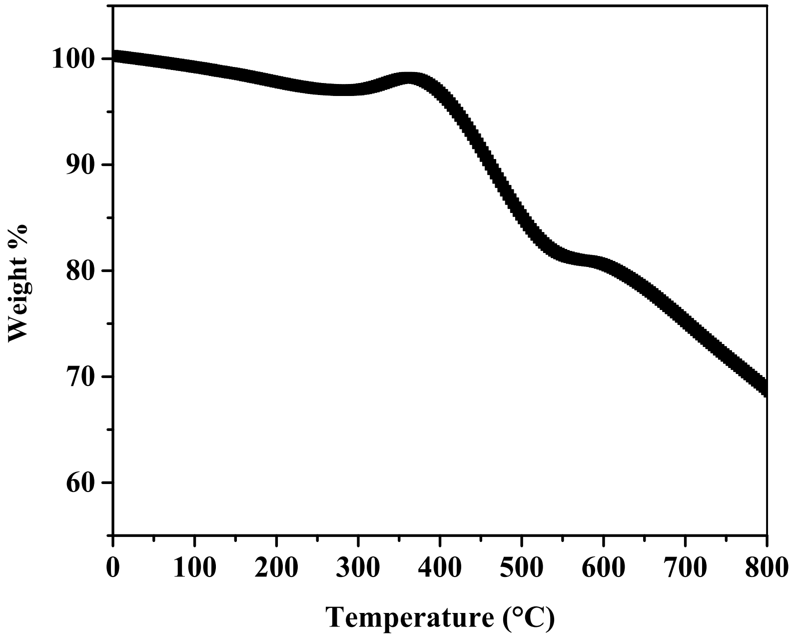

Fig. S9 TGA of compound **5.**

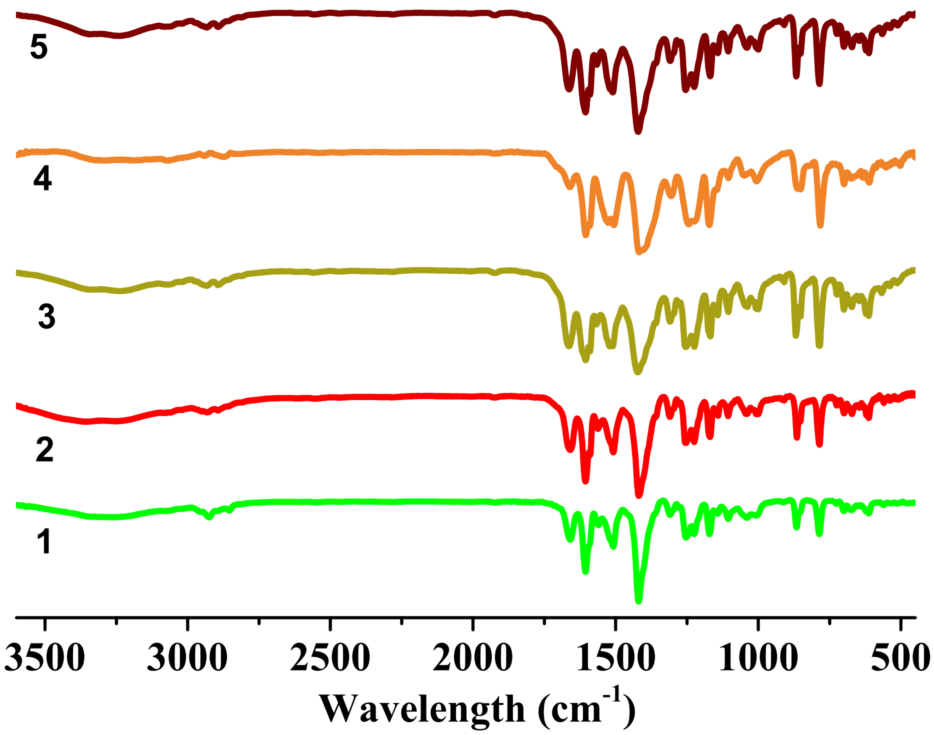

Fig.S10: FT-IR spectrum of **1, 2, 3, 4, 5 and 6**.

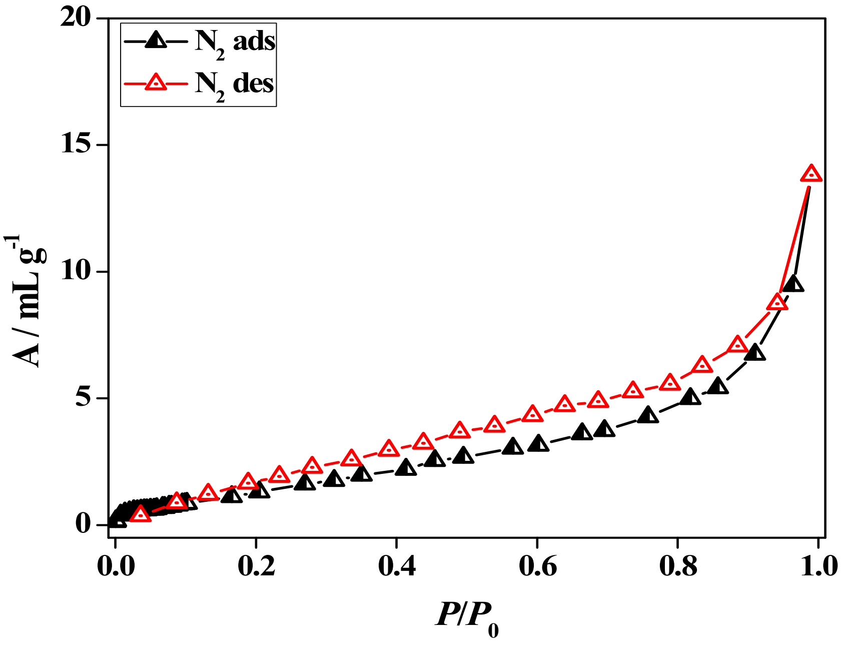

Fig.S11: N_2 adsorption isotherm of **2′** at 77 K.

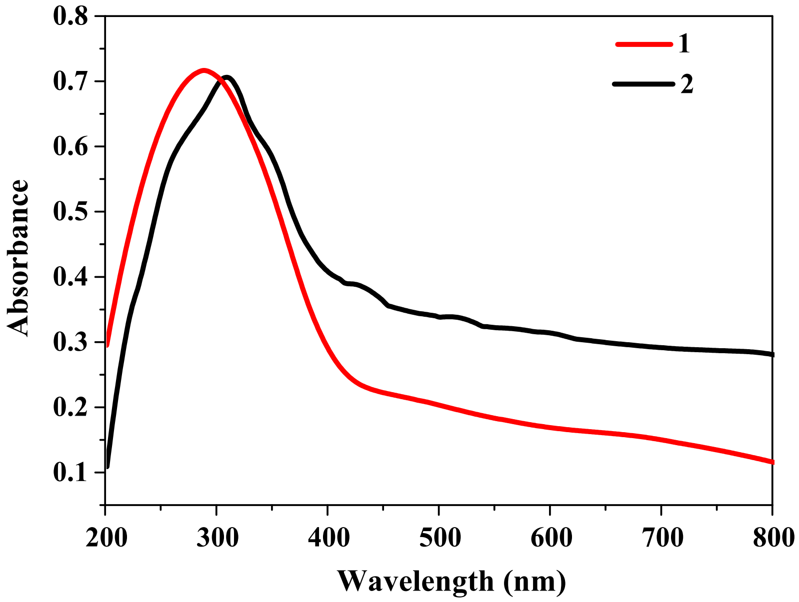

Fig.S12: UV-vis spectrum of **1** and **2**.

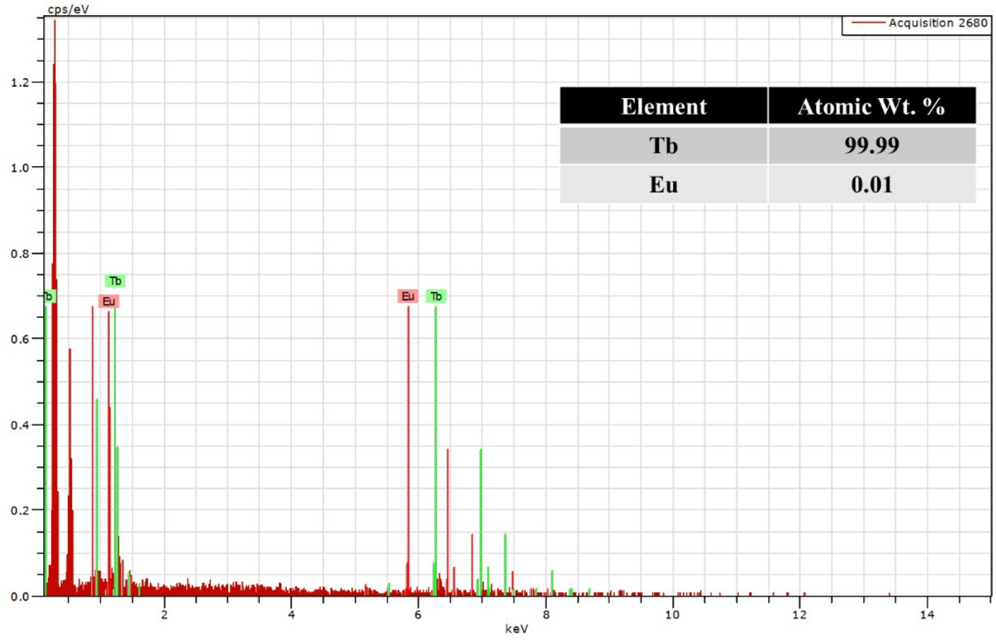

Element	Atomic Wt. %
Tb	99.99
Eu	0.01

Fig.S13: EDAX analysis of **1a**.

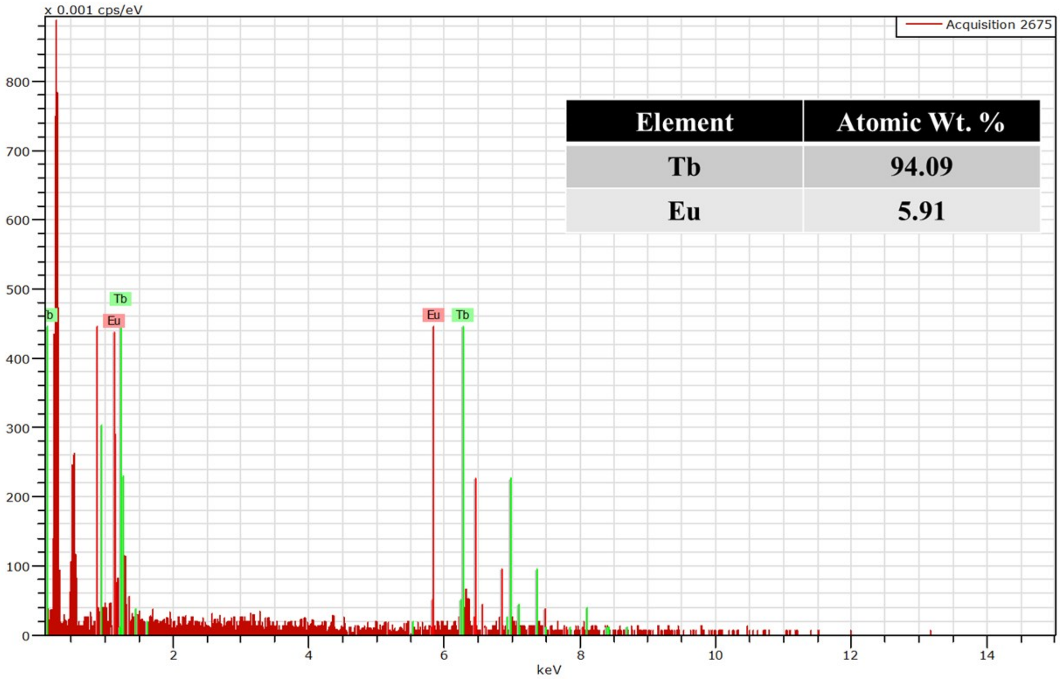

Element	Atomic Wt. %
Tb	94.09
Eu	5.91

Fig.S14: EDAX analysis of **1b**.

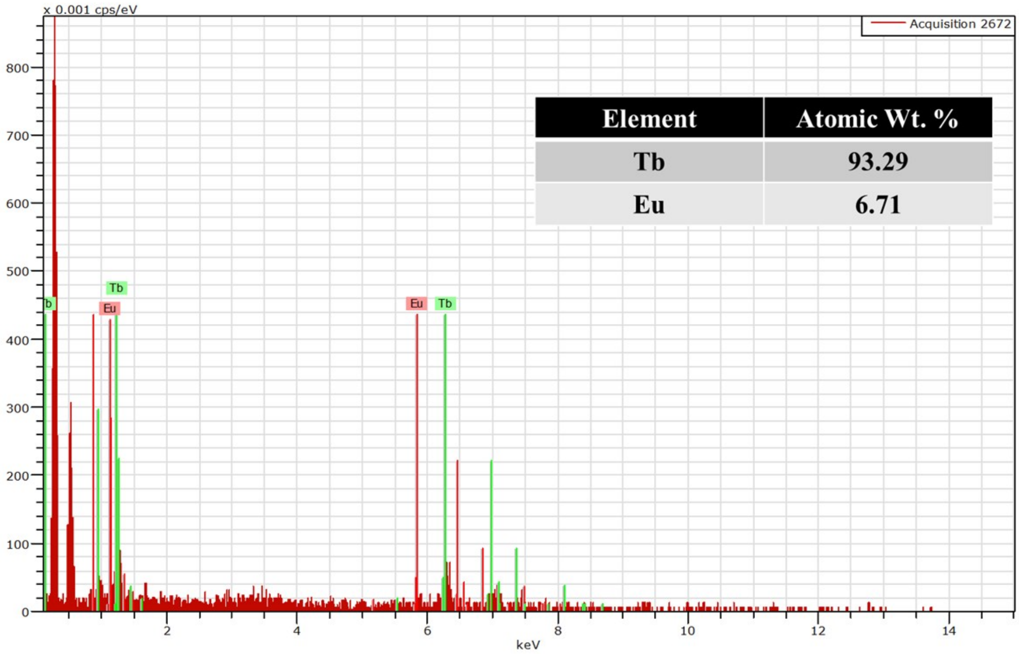

Element	Atomic Wt. %
Tb	93.29
Eu	6.71

Fig.S15: EDAX analysis of **1c**.

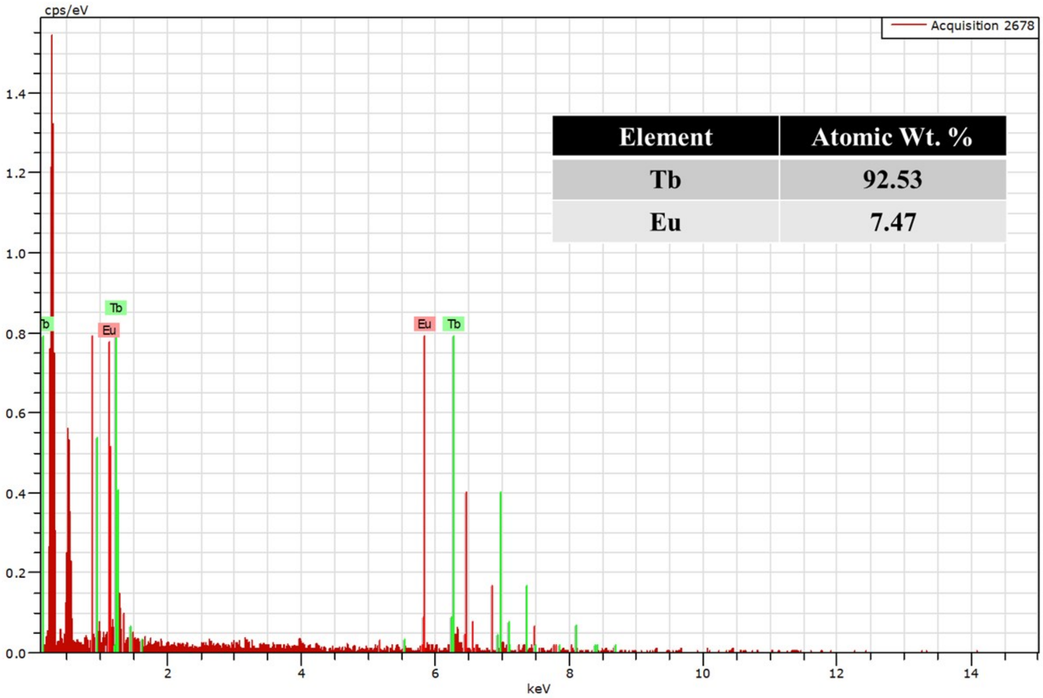

Element	Atomic Wt. %
Tb	92.53
Eu	7.47

Fig.S16: EDAX analysis of **1d**.

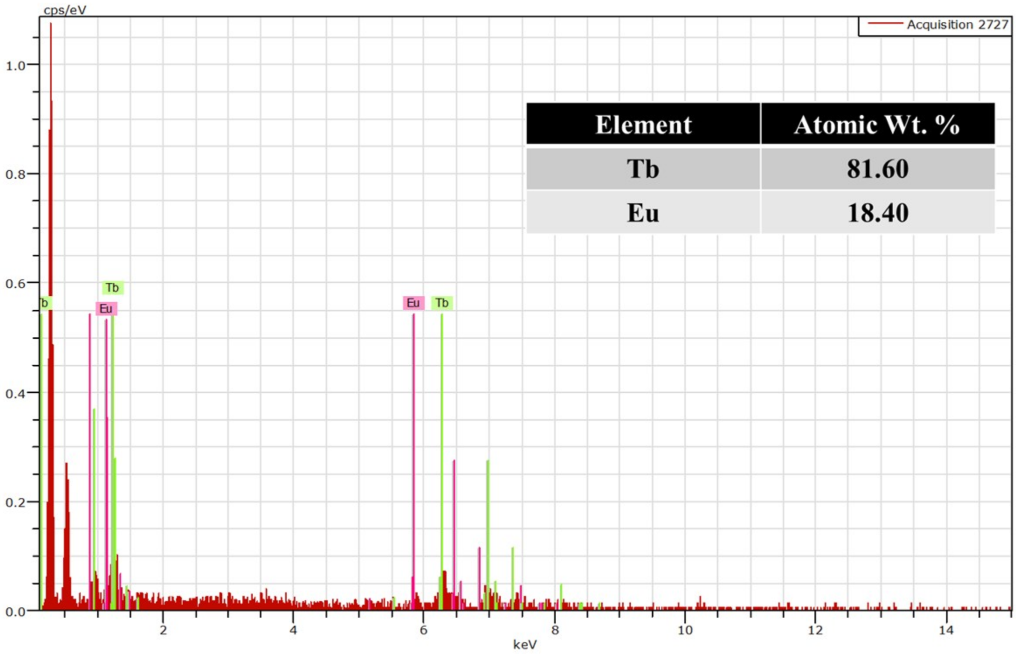

Element	Atomic Wt. %
Tb	81.60
Eu	18.40

Fig.S17: EDAX analysis of **1e**.

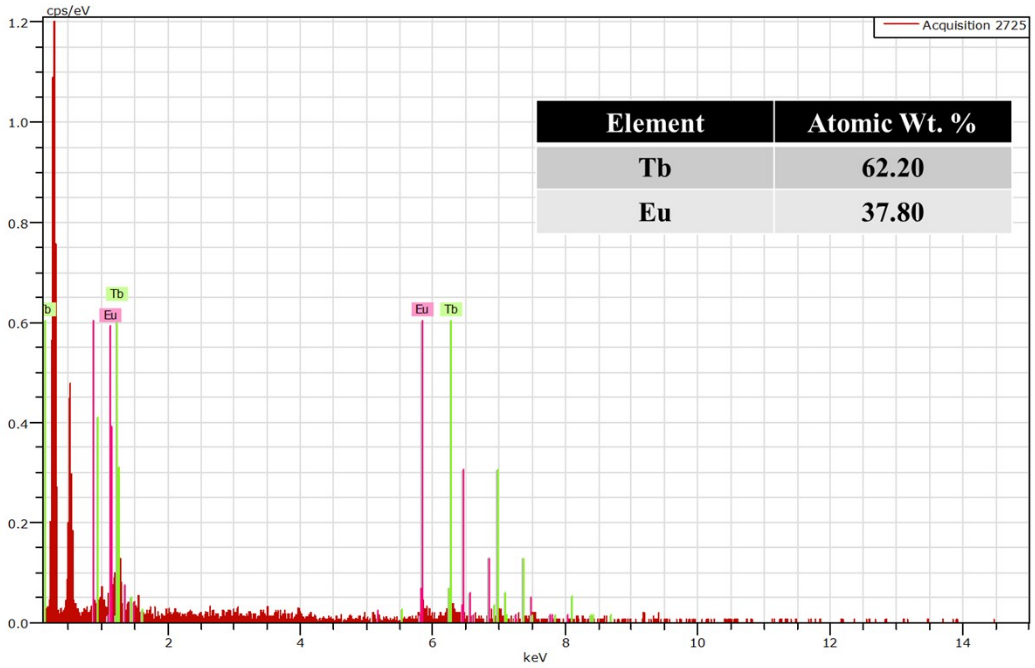

Element	Atomic Wt. %
Tb	62.20
Eu	37.80

Fig.S18: EDAX analysis of **1f**.

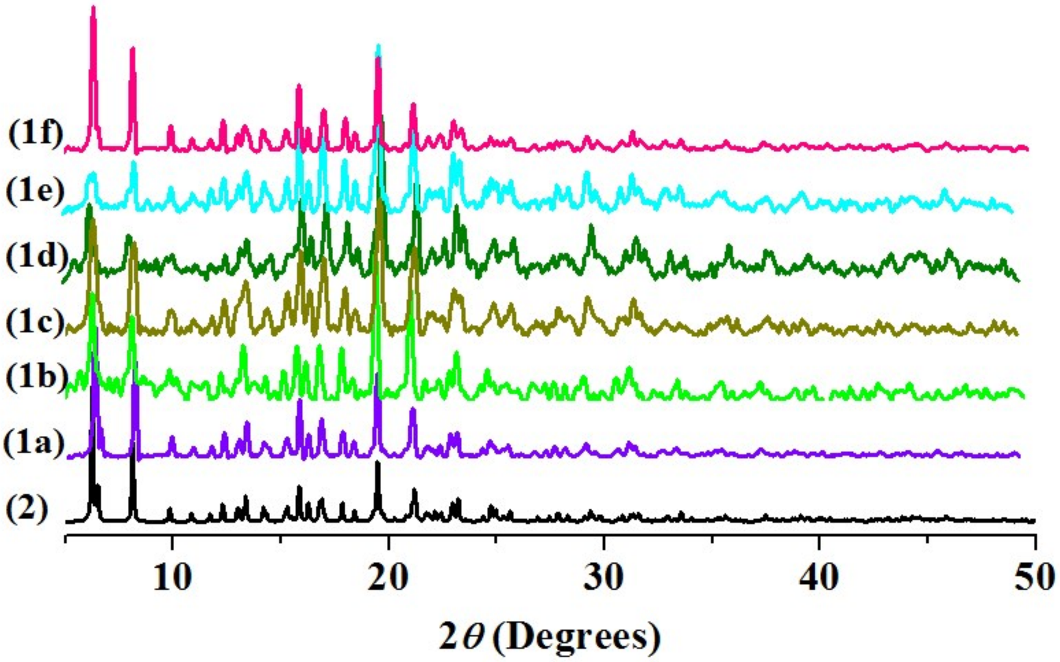

Fig.S19: PXRD patterns of as-synthesized compound **2** and **1a**-**1f**.

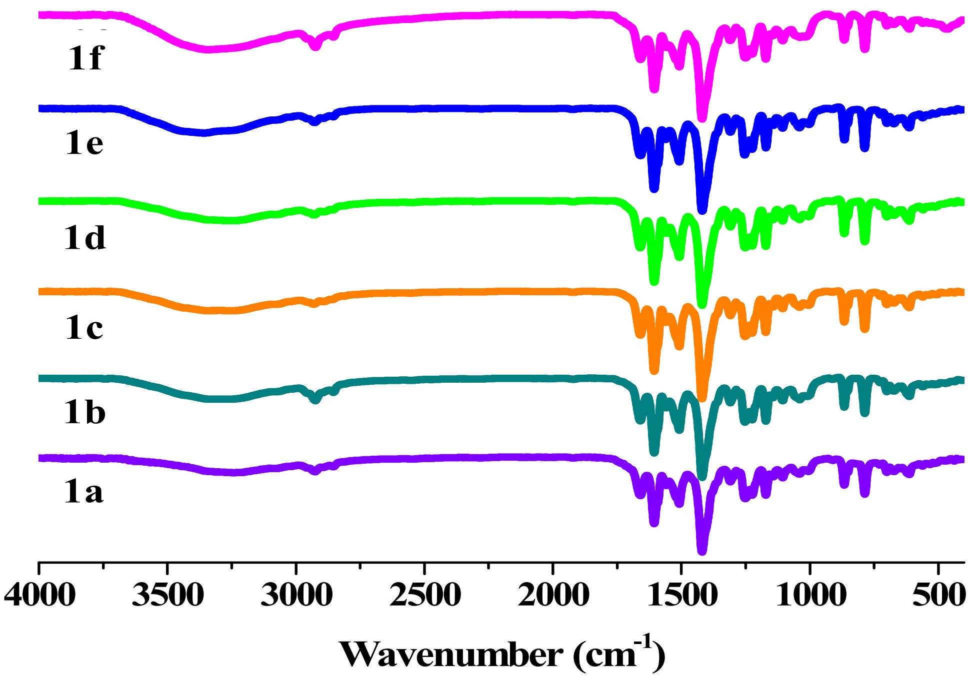

Fig.S20: FT-IR spectra of **1a-1f**.

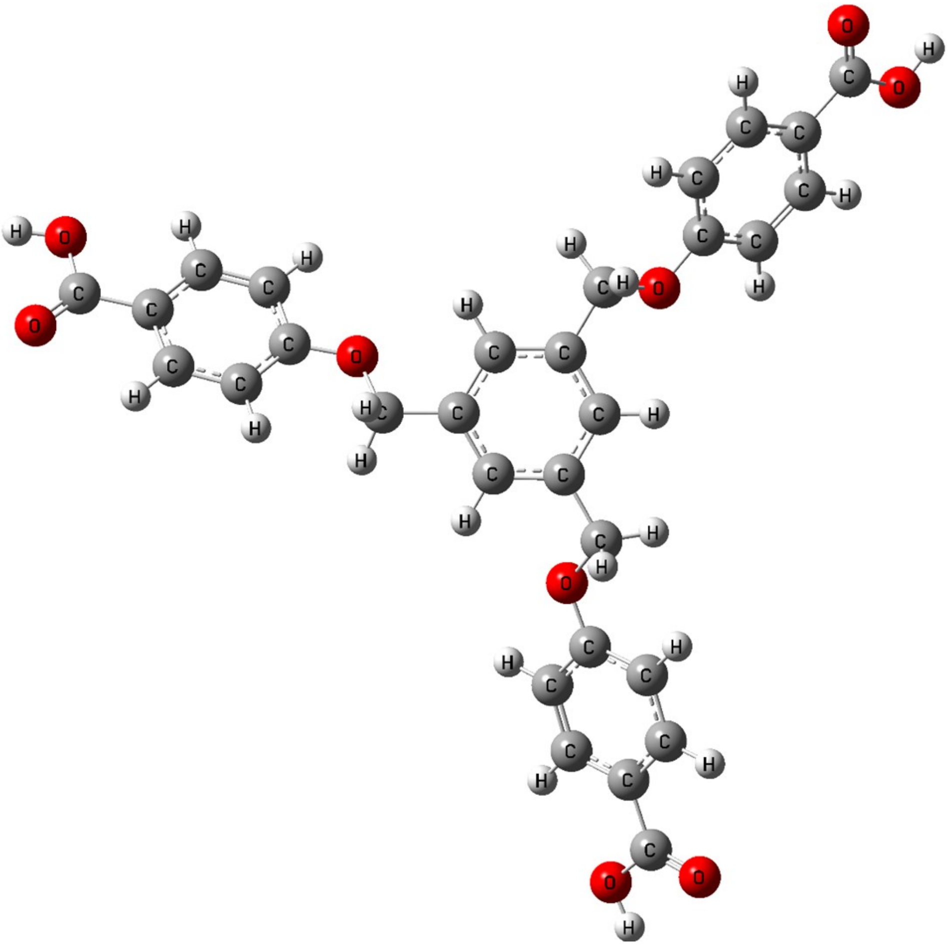

Fig S21. The optimized geometry of free ligand tri- at the B3LYP-D3/6-311++G(d,p) level.

Table S5: Summary of Time resolved photoluminescence decay of $^5D_4$ state of Tb^{III} in 1-1f at 544 nm

Sample	τ_1(ms)	τ_2(ms)	τ_3(ms)	B_1	B_2	B_3	τ_{av} (ms)
1	0.803	-	-	100%			0.803
1a	0.16	0.83	-	13.8 %	86.1 %	-	0.730
1b	0.14	0.74	-	10.3 %	89.6 %	-	0.680
1c	0.03	0.75	0.47	10.0 %	64.8 %	25 %	0.590
1d	0.01	0.33	0.7	16.1 %	9.3 %	74.4 %	0.550
1e	0.02	0.69	0.31	39.4 %	37.6 %	22.9 %	0.339
1f	0.01	0.1	0.71	41.1 %	16.3 %	42.5 %	0.327

Table S6: Summary of Time resolved photoluminescence decay of of $^5D_0$ state of Eu^{III} in 1a-1f at 614 nm.

Sample	τ_1(ms)	τ_2(ms)	τ_3(ms)	B_1	B_2	B_3	τ_{av} (ms)
1a	0.652	-	-	100%			0.652
1b	0.61	1.46	-	93.55 %	6.44 %	-	0.664
1c	1.00	0.62	-	12.74 %	87.25 %	-	0.668
1d	0.51	0.69	0.95	41.17 %	32.45 %	26.37 %	0.684
1e	0.59	0.68	1.8	48.05%	47.25%	4.68 %	0.689
1f	0.62	0.85	0.27	46.15 %	45.43 %	8.41 %	0.695

Calculation of energy transfer efficiency

The efficiency of energy transfer between donor and acceptor can be calculated from the luminescence lifetime of donor,

$$E= 1- \tau_{da} / \tau_d$$

τ_{da} and τ_d being the excited state lifetime of the donor in the presence and absence of acceptor respectively.

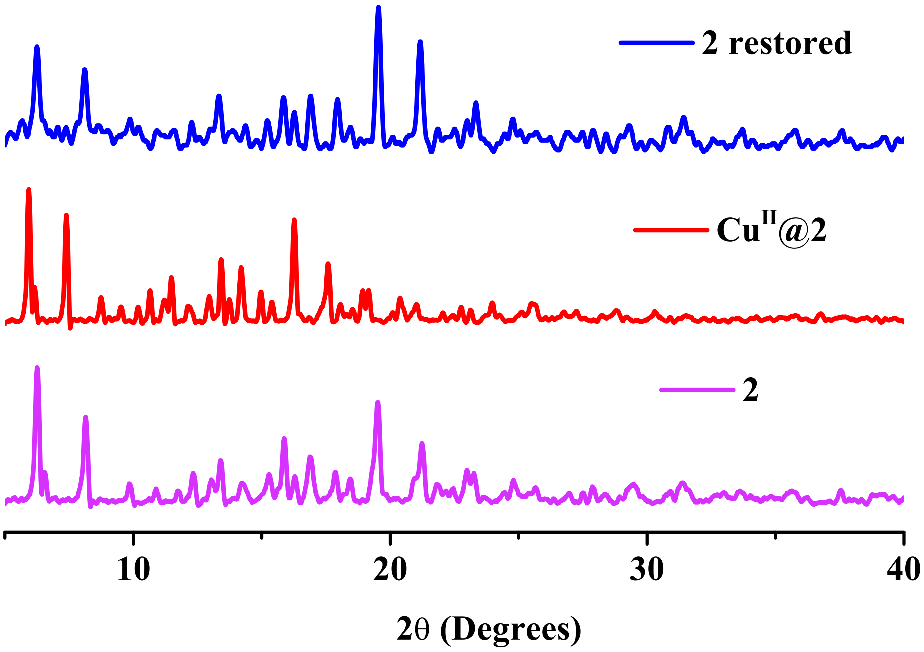

Fig S22. PXRD patterns of 2(pink), **Cu^{II}@2** (red), and recovered compound after treating **Cu^{II}@2** with EDTA (blue)

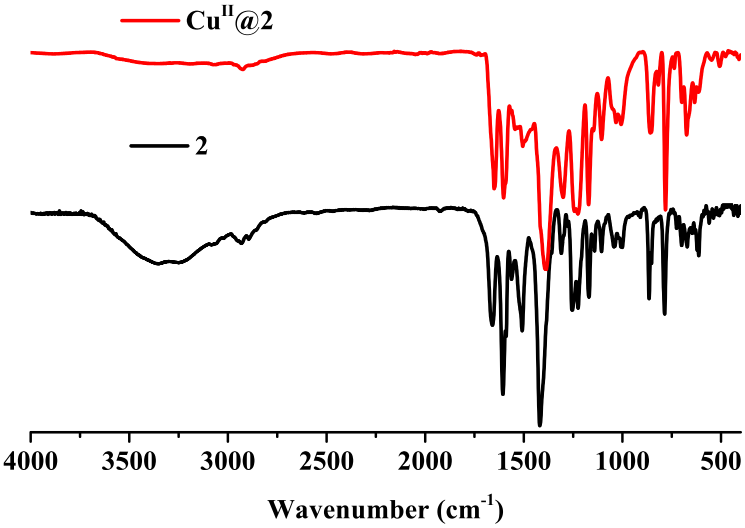

Fig S23. FT-IR spectra of **2** and **Cu^{II}@2.**

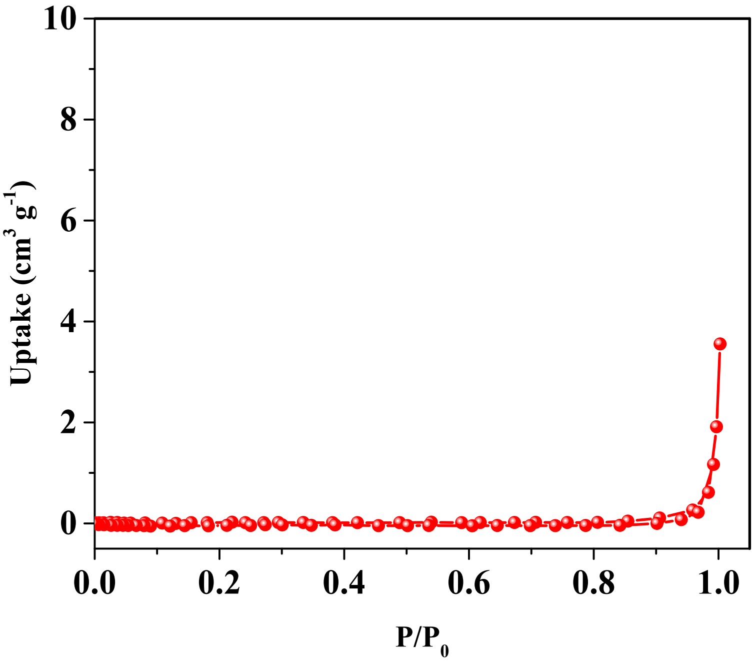

Fig S24 N_2 adsorption isotherm of **Cu^{II}@2** at 77

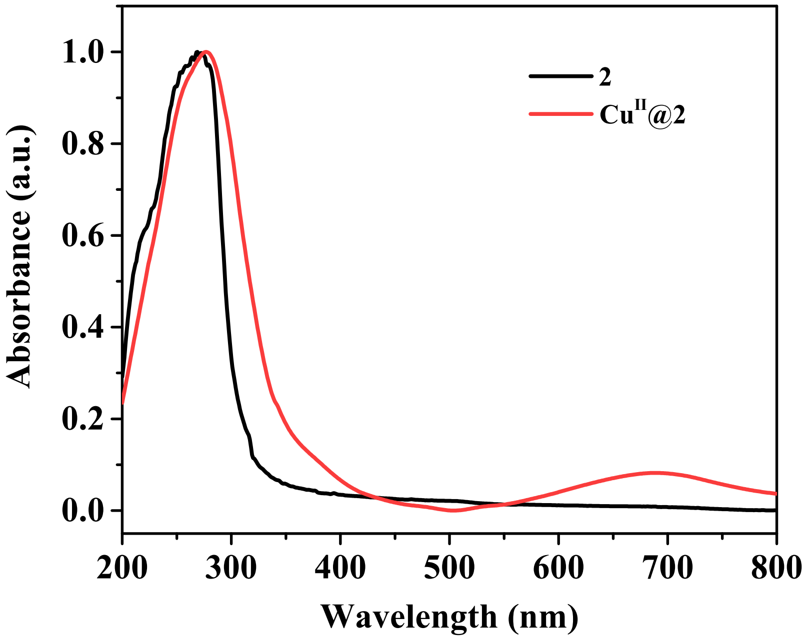

Fig S25. UV-vis spectra of **2** and **Cu^{II}@2**.

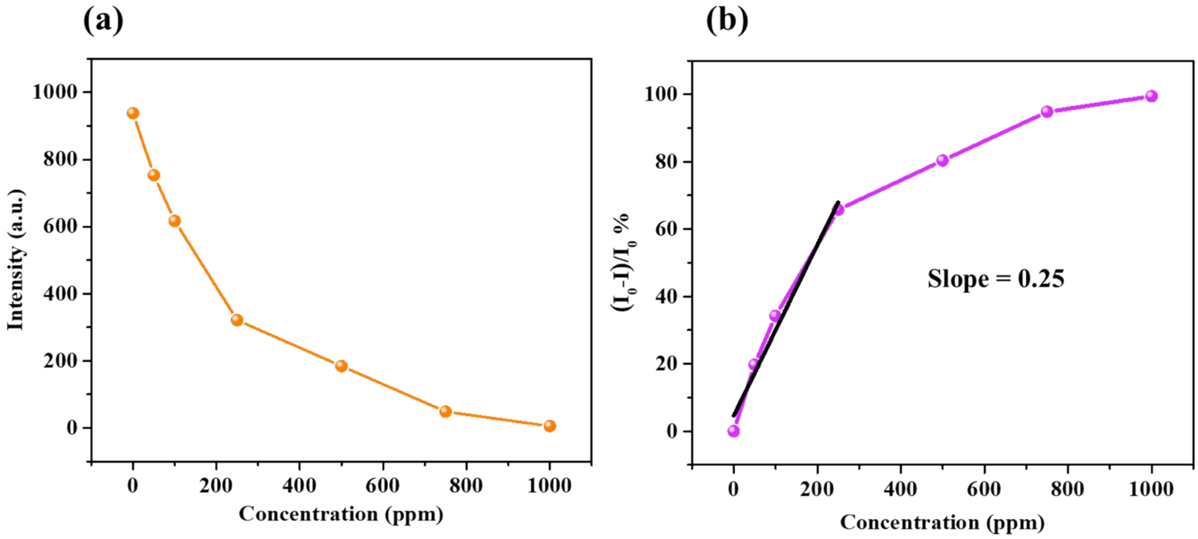

Fig S26.(a) Quenching of emission intensity of **2** upon increasing the concentration of Cu^{II}. **(b)** Plot for the calculation of limit of detection of Cu^{II}.

Excited State Calculation: All the calculations were performed under Density Functional Theory (DFT) model using the Gaussian 16 package of programs.[8] The molecular geometry of free ligand tri- was optimized using B3LYP-D3[9-14] exchange-correlation functional in conjunction with 6-311++G(d,p) basis set, as shown in Fig S27. The optimized structure (Table S5) was subjected to harmonic vibrational frequency calculation to confirm the nature of the stationary point. The effect of solvent was not considered to match with the solid-state experimental condition. Based on the optimized singlet ground state geometry, the energy of the triplet excited state of tri- ligand was calculated to be 3.3654 eV (27122 cm^{-1}) using the time-dependent DFT (TDDFT) approach. The pictures of the model structure of optimized free ligand tri- was taken from GaussView 6.0.16.[15]

Table S7: DFT-optimized singlet ground state geometry of free ligand tri-, computed at the B3LYP-D3/ 6-311++G(d,p) (HCO) level in absence of any solvent.

Atom	x	y	z
C	-0.19450400	-1.37869100	0.91158000
C	-1.29675700	-0.52988100	0.91036100
C	-1.09865000	0.85476500	0.90787600
C	0.18759600	1.38491700	0.91060200
C	1.28769800	0.52108100	0.91189200
C	1.10363000	-0.85789600	0.91456200
H	-0.33194000	-2.45383400	0.88412400
H	-1.96088400	1.51135800	0.87754900
H	2.28755500	0.93940300	0.88467500
C	2.29420900	-1.78067200	0.95515100
H	3.20284000	-1.24730100	0.65491400
H	2.44169100	-2.16293100	1.97398200
C	0.39057900	2.87771900	0.94741200
H	0.63712800	3.20051700	1.96768900
H	-0.52283100	3.39630900	0.63593800
C	-2.69105500	-1.10040500	0.94729900
H	-2.68314300	-2.15137000	0.63798700
H	-3.09469300	-1.04622300	1.96714700
O	2.05146400	-2.87928300	0.07045900
O	-3.52267800	-0.33402800	0.07028500
O	1.47202400	3.21423500	0.07257200
C	2.96963800	-3.87781100	-0.01220200
C	4.17987300	-3.90566600	0.69243500
C	2.63951100	-4.92979800	-0.87902200
C	5.04133900	-4.98449600	0.52667100
H	4.45833600	-3.10319200	1.36111900
C	3.50489000	-5.99732500	-1.03653500
H	1.70025000	-4.88118200	-1.41594500
C	4.71914000	-6.03751400	-0.33230500
H	5.98058200	-5.02076000	1.06497400
H	3.24735300	-6.80756400	-1.70587600
C	1.87736500	4.50866700	-0.01144400
C	2.96282200	4.74581100	-0.86731900
C	1.28752500	5.57332000	0.68176000
C	3.45530000	6.02871900	-1.02508800
H	3.39710900	3.90604000	-1.39556600
C	1.79181800	6.85849900	0.51582600
H	0.44599400	5.41545800	1.34174900
C	2.87432400	7.10300600	-0.33205900
H	4.29307400	6.20855100	-1.68586700
H	1.34694800	7.69208500	1.04543600
C	-4.84643100	-0.63012600	-0.01280200
C	-5.47340700	-1.67156900	0.68303200

C	-5.59465400	0.18938400	-0.87044400
C	-6.83856600	-1.87782100	0.51779100
H	-4.91577400	-2.31985500	1.34445300
C	-6.95195800	-0.02591600	-1.02746200
H	-5.08459500	0.98400400	-1.40080100
C	-7.59170800	-1.06457700	-0.33188000
H	-7.33789700	-2.67872400	1.04928600
H	-7.52666100	0.60802900	-1.68977900
C	3.36303600	8.49338800	-0.46361800
O	2.89894700	9.45383400	0.10912700
O	4.41883700	8.60716200	-1.31484100
H	4.66216500	9.54384700	-1.33349300
C	5.67931400	-7.15567800	-0.46313900
O	6.73708000	-7.23962200	0.11991300
O	5.25823500	-8.11943000	-1.32693600
H	5.94748500	-8.79882100	-1.34407300
C	-9.04018200	-1.33692900	-0.46254800
O	-9.63988200	-2.21723400	0.11302100
O	-9.66665400	-0.48224900	-1.31654400
H	-10.59950500	-0.73995300	-1.33436900

References:

1. *SMART (V 5.628), SAINT (V 6.45a), Xprep, SHELXTL; Bruker AXS Inc. Madison, Wisconsin, USA*, 2004.
2. *G. M. Sheldrick, Siemens Area Detector Absorption Correction Program, University of Götingen, Götingen, Germany*, 1994.
3. A. Altomare, G. Cascarano, C. Giacovazzo, A. Guagliardi, M. C. Burla, G. Polidori and M. Camalli, *J. Appl. Crystallogr.*, 1994, **27**, 435-435.
4. *G. M. Sheldrick, SHELXL-97, Program for Crystal Structure Solution and Refinement, University of Götingen, Götingen, Germany*, 1997.
5. A. L. Spek, *J. Appl. Crystallogr.*, 2003, **36**.
6. *L. J. Farrugia, WinGX-A Windows Program for Crystal Structure Analysis, J. Appl. Crystallogr.*

, 1999, **32**.
7. A. Chakraborty, K. K. Ramachandran, S. S. R. K. C. Yamijala, S. K. Pati and T. K. Maji, *RSC Adv.*, 2014, **4**, 35167-35170.
8. *M. J. Frisch, G. W. Trucks, H. B. Schlegel, G. E. Scuseria, M. A. Robb, J. R. Cheeseman, G. Scalmani, V. Barone, G. A. Petersson, H. Nakatsuji, X. Li, M. Caricato, A. V. Marenich, J. Bloino, B. G. Janesko, R. Gomperts, B. Mennucci, H. P. Hratchian, J. V. Ortiz, A. F. Izmaylov, J. L. Sonnenberg, D. Williams-Young, F. Ding, F. Lipparini, F. Egidi, J. Goings, B. Peng, A. Petrone, T. Henderson, D. Ranasinghe, V. G. Zakrzewski, J. Gao, N. Rega, G. Zheng, W. Liang, M. Hada, M. Ehara, K. Toyota, R. Fukuda, J. Hasegawa, M. Ishida, T. Nakajima, Y. Honda, O. Kitao, H. Nakai, T. Vreven, K. Throssell, J. A. Montgomery, Jr., J. E. Peralta, F. Ogliaro, M. J. Bearpark, J. J. Heyd, E. N. Brothers, K. N. Kudin, V. N. Staroverov, T. A. Keith, R. Kobayashi, J. Normand, K. Raghavachari, A. P. Rendell, J. C. Burant, S. S. Iyengar, J. Tomasi, M. Cossi, J. M. Millam, M. Klene, C. Adamo, R. Cammi, J. W. Ochterski, R. L. Martin, K. Morokuma, O. Farkas, J. B. Foresman and D. J. Fox, Gaussian 16, Revision A.03, Gaussian, Inc., Wallingford CT*, 2016.
9. K. Kim and K. D. Jordan, *J. Phys. Chem.*, 1994, **98**, 10089-10094.
10. P. J. Stephens, F. J. Devlin, C. F. Chabalowski and M. J. Frisch, *J. Phys. Chem.*, 1994, **98**, 11623-11627.
11. A. D. Becke, *Phys. Rev. A*, 1988, **38**, 3098-3100.

12. C. Lee, W. Yang and R. G. Parr, *Phys. Rev. B*, 1988, **37**, 785-789.
13. S. H. Vosko, L. Wilk and M. Nusair, *Can. J. Phys.*, 1980, **58**, 1200-1211.
14. A. D. Becke, *J. Chem. Phys.*, 1993, **98**, 5648-5652.
15. *R. Dennington, T. A. Keith and J. M. Millam, GaussView, Version 6.0.16, Semichem Inc., Shawnee Mission, KS*, 2016.